



Pulsed field ablation prevents chronic atrial fibrotic changes and restrictive mechanics after catheter ablation for atrial fibrillation

Yosuke Nakatani, Soumaya Sridi-Cheniti, Ghassen Cheniti, Francisco Daniel Ramirez, Cyril Goujeau, Clementine Andre, Takashi Nakashima, Charles Eggert, Christopher Schneider, Raju Viswanathan, et al.

► To cite this version:

Yosuke Nakatani, Soumaya Sridi-Cheniti, Ghassen Cheniti, Francisco Daniel Ramirez, Cyril Goujeau, et al.. Pulsed field ablation prevents chronic atrial fibrotic changes and restrictive mechanics after catheter ablation for atrial fibrillation. EP-Europace, 2021, 23 (11), pp.1767-1776. 10.1093/europace/euab155 . hal-03811670

HAL Id: hal-03811670

<https://hal.science/hal-03811670>

Submitted on 12 Oct 2022





HAL is a multi-disciplinary open access archive for the deposit and dissemination of scientific research documents, whether they are published or not. The documents may come from teaching and research institutions in France or abroad, or from public or private research centers.

L'archive ouverte pluridisciplinaire **HAL**, est destinée au dépôt et à la diffusion de documents scientifiques de niveau recherche, publiés ou non, émanant des établissements d'enseignement et de recherche français ou étrangers, des laboratoires publics ou privés.



Distributed under a Creative Commons Attribution - NonCommercial 4.0 International License

Pulsed field ablation prevents chronic atrial fibrotic changes and restrictive mechanics after catheter ablation for atrial fibrillation

Yosuke Nakatani ^{1*}, Soumaya Sridi-Cheniti², Ghassen Cheniti¹,
F. Daniel Ramirez ¹, Cyril Goujeau¹, Clementine André¹, Takashi Nakashima¹,
Charles Eggert³, Christopher Schneider³, Raju Viswanathan³, Philipp Krisai¹,
Takamitsu Takagi¹, Tsukasa Kamakura¹, Konstantinos Vlachos ¹,
Nicolas Derval^{1,4}, Josselin Duchateau^{1,4}, Thomas Pambrun^{1,4}, Remi Chauvel^{1,4},
Vivek Y. Reddy⁵, Michel Montaudon^{2,4}, François Laurent^{2,4}, Frederic Sacher^{1,4},
Mélèze Hocini^{1,4}, Michel Haïssaguerre^{1,4}, Pierre Jaïs^{1,4}, and Hubert Cochet ^{2,4}

¹Department of Cardiac Pacing and Electrophysiology, Hôpital Cardiologique du Haut-Lévêque, CHU de Bordeaux, Avenue de Magellan, 33604 Pessac, France; ²Department of Cardiovascular Imaging, Hôpital Cardiologique du Haut-Lévêque, CHU de Bordeaux, Pessac, France; ³Farapulse, Menlo Park, CA, USA; ⁴IHU LIRYC—CHU Bordeaux/Univ. Bordeaux/Inserm U1045, Pessac, France; and ⁵Department of Cardiac Arrhythmia, Icahn School of Medicine at Mount Sinai, New York, NY, USA

Received 4 October 2020; editorial decision 8 May 2021; accepted after revision 27 May 2021; online publish-ahead-of-print 8 July 2021

Aims

Pulsed field ablation (PFA), a non-thermal ablative modality, may show different effects on the myocardial tissue compared to thermal ablation. Thus, this study aimed to compare the left atrial (LA) structural and mechanical characteristics after PFA vs. thermal ablation.

Methods and results

Cardiac magnetic resonance was performed pre-ablation, acutely (<3 h), and 3 months post-ablation in 41 patients with paroxysmal atrial fibrillation (AF) undergoing pulmonary vein (PV) isolation with PFA ($n = 18$) or thermal ablation ($n = 23$, 16 radiofrequency ablations, 7 cryoablations). Late gadolinium enhancement (LGE), T2-weighted, and cine images were analysed. In the acute stage, LGE volume was 60% larger after PFA vs. thermal ablation ($P < 0.001$), and oedema on T2 imaging was 20% smaller ($P = 0.002$). Tissue changes were more homogeneous after PFA than after thermal ablation, with no sign of microvascular damage or intramural haemorrhage. In the chronic stage, the majority of acute LGE had disappeared after PFA, whereas most LGE persisted after thermal ablation. The maximum strain on PV antra, the LA expansion index, and LA active emptying fraction declined acutely after both PFA and thermal ablation but recovered at the chronic stage only with PFA.

Conclusion

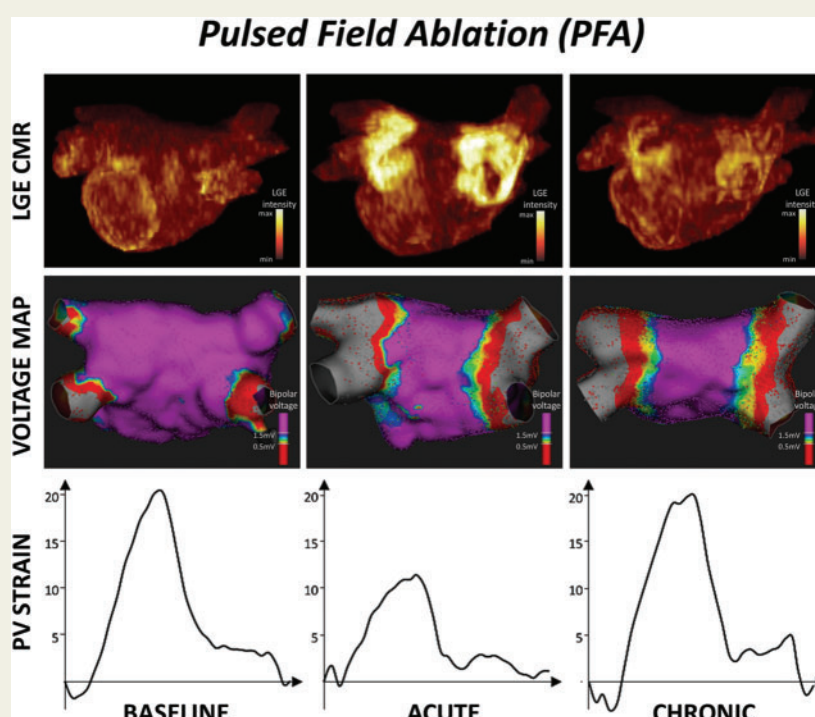
Pulsed field ablation induces large acute LGE without microvascular damage or intramural haemorrhage. Most LGE lesions disappear in the chronic stage, suggesting a specific reparative process involving less chronic fibrosis. This process may contribute to a preserved tissue compliance and LA reservoir and booster pump functions.

* Corresponding author. Tel: +33-5-57656542; fax: +33-5-57656509. E-mail address: yosuke3gbst@gmail.com

© The Author(s) 2021. Published by Oxford University Press on behalf of the European Society of Cardiology.

This is an Open Access article distributed under the terms of the Creative Commons Attribution Non-Commercial License (<http://creativecommons.org/licenses/by-nc/4.0/>), which permits non-commercial re-use, distribution, and reproduction in any medium, provided the original work is properly cited. For commercial re-use, please contact journals.permissions@oup.com

Graphical Abstract



Keywords

Atrial fibrillation • Catheter ablation • Pulsed field ablation • Cardiac magnetic resonance • Atrial fibrosis

What's new?

- In patients with paroxysmal atrial fibrillation, we compared left atrial (LA) structural and mechanical characteristics after pulsed field ablation (PFA) vs. thermal ablation by using cardiac magnetic resonance.
- As compared to thermal ablation methods, PFA induced larger acute late gadolinium enhancement (LGE) lesions, with no signs of microvascular obstruction or intramural haemorrhage.
- After PFA, the majority of acute LGE lesions had disappeared in the chronic stage, despite durable pulmonary vein isolation and low voltage areas.
- The wall compliance acutely declined in PFA lesions, but recovered in the chronic stage, leading to a recovery of LA reservoir and booster pump functions.

necrosis, which acutely combines oedema, intramural haemorrhage, and microvascular damage.¹ In the chronic stage, acute lesions transform into areas of reparative fibrosis, which makes post-ablation scar tissue poorly compliant. Massive fibrosis impairs the left atrial (LA) reservoir function² and is associated with specific complications, including PV stenosis³ and stiff LA syndrome.⁴ Recently, pulsed field ablation (PFA) has been introduced as a new energy source. Pulsed field ablation is a non-thermal ablative modality in which high voltage ultra-short pulses are applied to target tissue. Pulsed field ablation destabilizes cell membranes by forming irreversible nanoscale pores, driving a leakage of cell contents leading to cell death.^{5,6} With PFA, lesions are homogeneous, while preserving the extracellular matrix architecture, nerves, and microvascular structures.^{7,8} However, the impact of PFA on the atrial tissue composition and subsequent mechanics has never been studied in patients. This study aimed to compare LA structural and mechanical characteristics after PFA vs. thermal ablation, by using cardiac magnetic resonance (CMR).

Introduction

Pulmonary vein (PV) isolation has become the cornerstone technique for catheter ablation in patients with drug-refractory atrial fibrillation (AF). At present, almost all ablation technologies are mediated by a thermal effect. Thermal methods induce coagulative

Methods

Study population and protocol

The subjects of this study were patients with paroxysmal AF, who underwent a first catheter ablation procedure at Bordeaux University Hospital

(Bordeaux-Pessac, France), with no contra-indication to gadolinium-enhanced CMR. Patients treated with PFA (PFA group) were a part of IMPULSE (A Safety and Feasibility Study of the IOWA Approach Endocardial Ablation System to Treat Atrial Fibrillation) (NCT03700385) and PEFCAT (A Safety and Feasibility Study of the FARAPULSE Endocardial Ablation System to Treat Paroxysmal Atrial Fibrillation) (NCT03714178) trials. In these trials, we prospectively enrolled patients who underwent PFA from October 2018 to November 2019. Patients treated with thermal ablation (thermal group) were prospectively included, from February 2019 to November 2019, from the cohort of patients undergoing a first AF ablation with radiofrequency ablation or cryoablation in our institution. The inclusion criteria were similar to those of the PFA group, although patients were not consecutive because the inclusion depended on the availability of the CMR system at the end of the procedure. In both groups, CMR was performed at baseline (within 4 days before ablation), in the acute stage (less than 3 h post-ablation), and in the chronic stage (3-month follow-up). In the PFA group, repeat electrophysiological mapping was performed at 3 months to assess PV isolation durability. A total of 18 patients were included in the PFA group, and 23 patients in the thermal group, including 16 patients with RF ablation, and 7 with cryoablation. The study was approved by the Institutional Ethical Committee, and all patients gave informed consent.

Catheter ablation

All procedures were performed under conscious sedation and uninterrupted oral anticoagulation. In all patients, the procedural endpoint was PV isolation.

In the PFA group, a 12-Fr over-the-wire PFA ablation catheter (Farawave, Farapulse, Inc., Menlo Park, CA, USA) with five splines, each containing four electrodes, was deployed in either a flower petal or basket configuration, depending on PV anatomy. The catheter was advanced over a guidewire such that the splines achieve circumferential contact/proximity with the PV antra. The ablation protocol underwent consecutive evolutionary modifications: from monophasic to biphasic pulses, and then optimizing the biphasic waveform morphology and pulse sequence composition. With the latest waveform (the commercially approved waveform) used in PEFCAT, the energy was delivered in a set of micro-second-scale biphasic pulses of 1800–2000 V in bipolar fashion across all electrodes, and one application was made of five pulse packets delivered over a few seconds. Details on other PFA protocols were described in the previous report.⁶ In the present study, all patients were treated with biphasic pulses. Ten patients were treated with the latest waveform (Biphasic 3), and the other eight patients were treated with the second version of the biphasic waveform (Biphasic 2).⁶ Applications were repeated eight times per vein, with repositioning and/or rotation of the catheter every two applications to ensure circumferential PV ostial and antral coverage. As a part of IMPULSE and PEFCAT protocols, a 3D mapping system (CARTO, Biosense Webster, Inc., Diamond Bar, CA, USA; or RHYTHMIA, Boston Scientific, Marlborough, MA, USA) was used to acquire baseline and post-ablation voltage maps. Sequential contact mapping was performed with a multi-electrode mapping catheter (PENTARAY, Biosense Webster, Inc.; or ORION, Boston Scientific). Besides, repeat 3D mapping was performed to assess the durability of PV isolation at 3 months.

In patients undergoing RF ablation, PV isolation was performed using the CARTO system, with an irrigated tip RF catheter with a contact force sensor (Thermocool Smarttouch SF, Biosense-Webster, Inc.). We delivered RF during 15–30 s applications, with a temperature limited to 52°C and a maximum power of 45 W.

In patients undergoing cryoablation, PV isolation was performed using a 28-mm cryoballoon catheter (Arctic Front Advance, Medtronic,

Minneapolis, MN, USA), under fluoroscopic guidance. The occlusion of PV was confirmed with the retention/leakage of the contrast agent after injection at the balloon's distal tip. A minimum of two freezes were delivered to each PV with a targeted duration of 180 s.

After PV isolation, the entrance block was confirmed by placing an electrode catheter within the PVs, and the exit block by pacing from the catheter.

Cardiac magnetic resonance acquisition

Cardiac magnetic resonance studies were conducted on a 1.5 T system (MAGNETOM AERA[®], Siemens Medical Systems, Erlangen, Germany). The imaging protocol comprised cine SSFP imaging in a two-chamber view as well as in a stack of contiguous four-chamber views covering the entire LA. Black-blood T2-weighted imaging was acquired in a stack of contiguous four-chamber views covering the entire LA using a T2 SPAIR sequence performed before contrast injection. Atrial late gadolinium enhancement (LGE) imaging was initiated 20 min after the intravenous injection of 0.2 mmol/kg gadoterate meglumine (Guerbet, Aulnay-sous-bois, France). Imaging was acquired in trans-axial orientation at a mid-diastolic phase using a 3D, inversion-recovery-prepared, ECG-gated, respiration-navigated gradient-echo pulse sequence with fat-saturation.⁹

Cardiac magnetic resonance analysis

Cardiac magnetic resonance analysis was performed by a single observer with 15 years of experience in CMR. The analysis was blinded from clinical and procedural characteristics. Left atrial tissue characteristics were analysed in the total population, while LA volume, phasic function, and strain were only analysed in a subset of the population whose cine images fulfilled the following criteria: (i) imaging acquired in sinus rhythm at all time points, (ii) consistent slice positioning across the three CMR studies, and (iii) comprising comparable four-chamber cine views at the level of right and left PV antra.

Left atrial tissue characteristics on T2 and LGE images were analysed using MUSIC Software (IHU Liryc, Univ. Bordeaux—Inria Sophia Antipolis, France). The LA wall was manually segmented on the baseline, acute, and chronic LGE images, as well as on acute T2-weighted images. On baseline LGE images, LA fibrosis was segmented by adaptive thresholding of myocardial voxels as described previously.⁹ Fibrosis burden was expressed in % of the LA wall. The reproducibility of baseline LGE quantification can be found in our prior publication.¹⁰

Acute LGE images were reviewed by one expert observer blinded to patient characteristics and particularly to the ablation technique. Dark areas within LGE suggestive of microvascular damage or intra-mural haemorrhage¹¹ were described as present or absent. After manual segmentation of the LA wall, acute, and chronic post-ablation LGE was quantified by applying the full width at half maximum method,¹² thus taking the maximum signal intensity as an internal reference and a threshold set at 50% maximum intensity. The total volume of LGE throughout the atrial wall was expressed in mL. The reproducibility of post-ablation LGE quantification can be found in one prior publication.² Acute tissue oedema was quantified from T2 SPAIR images by using manual histogram thresholding. After manual segmentation of the atrial wall on contiguous T2 SPAIR images covering the entire LA, the histogram of voxels intensities within the wall was displayed. The expert blinded to patient characteristics, particularly the ablation technique, manually set a threshold to best segment hyperintense areas with the image. The optimization of the threshold was assisted by real-time visualization of the resulting segmentation overlaid on the original image when varying the threshold. The total volume of oedema on T2 imaging was expressed in mL.

Left atrial volume and phasic function were analysed using CMR42 software (Circle Cardiovascular Imaging Inc., Calgary, Canada). Semi-

Table 1 Patients' baseline characteristics

	All patients (n = 41)	PFA group (n = 18)	Thermal group (n = 23)	P-value
Demographics				
Age (years)	58 ± 9	56 ± 9	60 ± 8	0.146
Male gender	32 (78)	15 (83)	17 (74)	0.470
Comorbidities				
Structural heart disease	4 (10)	2 (11)	2 (9)	0.598
Congestive heart failure	1 (2)	0 0	1 (4)	0.561
Left ventricular ejection fraction (%)	61 ± 7	62 ± 6	61 ± 8	0.500
Body mass index (kg/m ²)	26 ± 4	26 ± 4	26 ± 3	0.766
Hypertension	8 (20)	4 (22)	4 (17)	0.698
Diabetes mellitus	1 (2)	1 (6)	0 0	0.439
Past history of stroke or TIA	2 (5)	1 (6)	1 (4)	0.691
Vascular disease	3 (7)	1 (6)	2 (9)	0.593
CHA ₂ DS ₂ -Vasc score	1 [0–1]	0.5 [0–1]	1 [0–1]	0.731
Medications				
Warfarin	2 (5)	0 0	2 (9)	0.309
Direct oral anticoagulant	39 (95)	18 (100)	21 (91)	0.200
Aspirin	1 (2)	1 (6)	0 0	0.439
Antiarrhythmic drug	31 (76)	13 (72)	18 (78)	0.655
Beta-blocker	17 (41)	8 (44)	9 (39)	0.732
LA structure/function				
LA fibrosis on baseline LGE (%)	17.0 ± 3.5	16.7 ± 3.4	17.3 ± 3.7	0.546
Maximum LA volume (mL) ^a	77 [68–84]	76 [64–84]	77 [70–85]	0.561
Pre-contraction LA volume (mL) ^a	59 [50–67]	57 [46–66]	60 [57–68]	0.360
Minimum LA volume (mL) ^a	31 [25–44]	30 [24–44]	39 [28–46]	0.406
LA ejection fraction (%) ^a	58 [43–65]	58 [48–66]	55 [41–65]	0.678
LA expansion index (%) ^a	136 [76–185]	136 [94–194]	123 [68–189]	0.678
LA active emptying fraction (%) ^a	40 [30–54]	41 [30–54]	40 [30–52]	0.967
Maximum global strain 2C (%) ^a	16 [12–21]	16 [10–25]	16 [11–24]	0.967
Maximum global strain 4C (%) ^a	15 [9–21]	16 [10–25]	11 [8–21]	0.339

Data are mean ± SD, median [interquartile range Q1–Q3], or number (%) of patients.

^aMeasured in 30 patients (16 from PFA group and 14 from the thermal group) with appropriate cine images.

2C, 2-chamber; 4C, 4-chamber; LA, left atrium; LGE, late gadolinium enhancement; PFA, pulsed field ablation; TIA, transient ischaemic attack.

automated LA segmentation and contour propagation were applied on two-chamber and four-chamber cine images, and the LA volume was computed at each time point using the biplane area-length method. From the maximum, minimum, and pre-LA contraction volumes, the LA ejection fraction, LA expansion index, and LA active emptying fraction were computed as described previously.²

Left atrial strain was assessed by a cine CMR-based deformation registration algorithm (TruFiStrain, Siemens Healthcare, Medical Imaging Technologies, Princeton, NJ, USA). This algorithm allows for myocardial strain computation on a pixel basis with high reproducibility.¹³ After tracing the LA endocardium, longitudinal strain curves were automatically computed on pre-defined LA segments. The maximum strains of the LA septum, posterior wall, lateral wall, and right and left PV antra were measured from a four-chamber view, whereas those of the LA roof and bottom wall were measured from a two-chamber view. Global LA strain in two-chamber and four-chamber views were also assessed.

Follow-up

Patients were followed at 1 month, 3 months, and every 6 months thereafter. A 12-lead surface ECG was performed at each visit, and 24-h

Holter monitoring was performed in case of symptoms. Arrhythmia recurrence was defined as AF and atrial tachycardia episodes lasting ≥30 s. Arrhythmias occurring in the first 3 months after the ablation (blanking period) was censored.

Statistical analysis

The Shapiro–Wilk test of normality was used to assess whether quantitative data conformed to the normal distribution. Continuous data are expressed as mean ± standard deviation when following a normal distribution, and as median [interquartile range Q1–Q3] otherwise. Categorical data are expressed as number (%). Independent continuous variables were compared using independent-sample parametric (unpaired Student's *t*-test) or non-parametric tests (Mann–Whitney *U* test) depending on data normality. Independent categorical variables were compared using the Chi-square test when expected frequencies were ≥5, and Fisher's exact test when they were <5. Besides, the changes of parameters were analysed using two-way repeated-measures analysis of variance. If significant changes were observed, post hoc tests with Bonferroni-adjusted pairwise comparisons were performed. We considered *P* < 0.050 as statistically significant.

Table 2 Procedural characteristics and outcomes

	All patients (n = 41)	PFA group (n = 18)	Thermal group (n = 23)	P-value
Fluoroscopy time (min)	23 [18–29]	23 [17–29]	20 [18–31]	0.796
Total procedure time (min)	111 [95–146]	96 [77–111]	130 [110–200]	0.001
Total number of PFA applications	NA	32 [32–37]	NA	NA
Total ablation time (min)	NA	<1	RF 37 [26–72] CRYO 16 [15–20]	NA
Successful PV isolation	41 (100)	18 (100)	23 (100)	>0.999
Complication	3 (7)	1 (6)	2 (9)	>0.999
PV reconnection at 3 months remap	NA	0/0	NA	NA
Follow-up duration	9 ± 4	9 ± 3	9 ± 4	0.972
Arrhythmia recurrence	11 (27)	2 (11)	9 (39)	0.098

Data are median [interquartile range Q1–Q3] or number (%) of patients.

CRYO, cryoablation; PFA, pulsed field ablation; PV, pulmonary vein; RF, radiofrequency.

Results

Baseline patients' characteristics

Patient baseline characteristics are summarized in *Table 1*. The mean age was 58 ± 9 years, and 78% of patients were male. Maximum LA volume was $77 [68–84]$ mL, and LA fibrosis on baseline LGE imaging was $17.0 \pm 3.5\%$ of the LA wall. No significant difference in patients' characteristics was observed between the PFA group and the thermal group.

Procedure characteristics and outcomes

Procedural characteristics are summarized in *Table 2*. Total procedure time was significantly shorter in the PFA group than in the thermal group [$96 (77–111)$ min vs. $130 (110–200)$ min, $P = 0.001$]. In the PFA group, the total energy delivery time was consistently <1 min. PV isolation was completed in all patients. Groin haematomas were observed in one patient of the PFA group and two patients of the thermal group, all resolving with conservative therapy. Over a comparable follow-up duration (9 ± 3 months vs. 9 ± 4 months, $P = 0.972$), atrial arrhythmia recurred in two patients from the PFA group (two AF episodes), vs. nine patients from the thermal group (seven AF and two atrial tachycardias). Arrhythmia free survival rate tended to be higher in the PFA group than in the thermal group (log-rank, $P = 0.098$). Notably, no PV reconnection was observed in the PFA group on the repeat mapping study at 3 months.

Changes in tissue characteristics

Cardiac magnetic resonance imaging was performed in sinus rhythm at all time points in all patients, except for one RF-treated patient who underwent acute CMR in AF. No patient showed LGE and tissue oedema at baseline. The burdens of acute and chronic LGE and acute tissue oedema are shown in *Figure 1*. On acute CMR, all patients showed LGE on the antrum or ostium of all PVs. LGE was 60% larger after PFA than after thermal ablation (16.1 ± 2.5 mL vs. 10.1 ± 2.3 mL, $P < 0.001$). After PFA, tissue changes on LGE were dense and homogeneously distributed around PV antra, and signs of microvascular damage or intramural haemorrhage were observed in none of the patients. In contrast, after thermal ablation, LGE sites

were composed of a mix of hyper-enhanced and dark areas in all patients ($P < 0.001$ vs. PFA), suggestive of intramural haemorrhage and/or microvascular damage. Acute tissue oedema was observed in both groups, although slightly less in the PFA group than in the thermal group (10.0 ± 1.5 mL vs. 12.0 ± 2.1 mL, $P = 0.002$). Examples of acute tissue changes on LGE and T2 imaging are illustrated in *Figure 2*. In the chronic stage, the majority of the LGE observed acutely had disappeared in the PFA group (mean LGE reversibility $60 [55–65]\%$ of acute values), whereas this reversibility of LGE was much less observed in the thermal group ($18 [12–34]\%$, $P < 0.001$ vs. PFA), with the majority of the LGE persisting (*Figure 3*). Importantly, although LGE reversibility was observed in all patients after PFA, none of them showed PV reconnection at 3-month remapping, and low voltage areas around PVs remained unchanged, as illustrated in *Supplementary material* online, *Figure S1*.

Changes in left atrial strain

Cine images were deemed appropriate for analysis in a subset of 30 patients (16 PFA, 8 RF ablations, and 6 cryoablations). Changes in maximum longitudinal strain values on the PV antra are shown in *Figure 4*. The maximum strain on the right PV antra showed an acute decline after both PFA and thermal ablation ($P < 0.001$ and $P = 0.002$, respectively). However, it recovered to the baseline level at 3 months in the PFA group ($P < 0.001$ for acute vs. chronic), while it stayed altered in the thermal group. Similar results were observed on the left PV antra. Examples of strain measurements are shown in *Figure 5*. The maximum strain on the septum declined after 3 months in the thermal group while it did not change after PFA. Likewise, the maximum strain on the posterior wall recovered at 3 months in the PFA group, but not after thermal ablation. No significant changes in maximum strain were observed in the other LA areas. Consequently, the global LA strain did not significantly change throughout the protocol.

Changes in left atrial volume and function

Changes in LA volume and function are shown in *Figure 6*. In both groups, the LA volume tended to decrease between each time point,

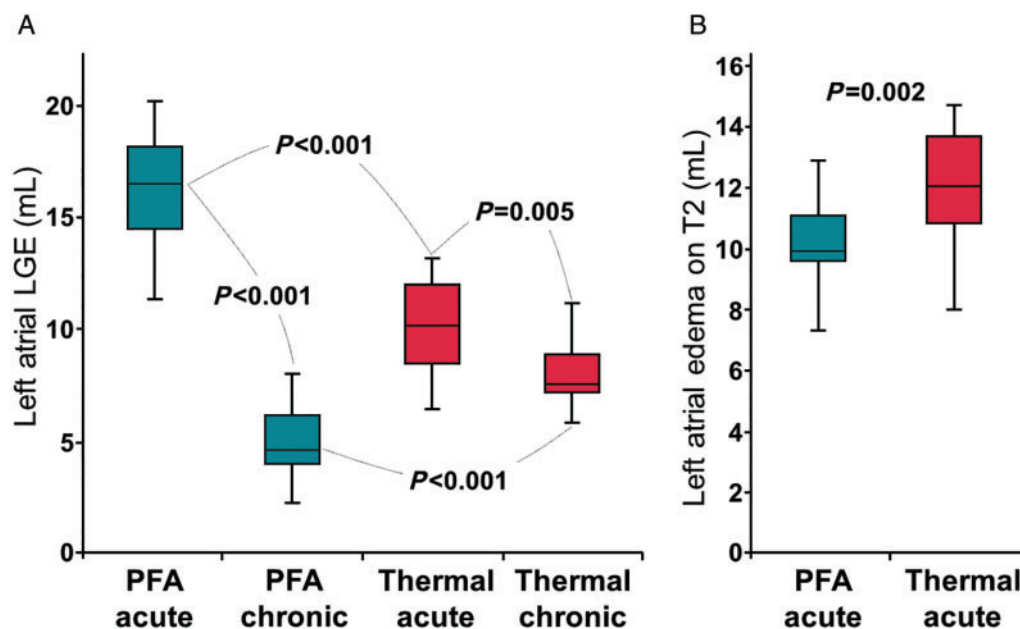


Figure 1 The burdens of acute and chronic late gadolinium-enhancement (LGE) and acute oedema. (A) Left atrial (LA) LGE lesions in acute and chronic stages. (B) LA oedema on hyper-T2 imaging in the acute stage. PFA, pulsed field ablation.

while the LA ejection fraction acutely declined before going back to baseline values at 3 months. The LA expansion index declined in both groups in the acute stage. In the chronic stage, it remained altered in the thermal group while recovered in the PFA group. A similar result was observed on the LA active emptying fraction.

Discussion

The main findings are as follows. First, PFA induced larger acute LGE than thermal ablation. Second, acute tissue changes after PFA were homogeneous without signs of microvascular obstruction or intramural haemorrhage, while this was constantly observed after thermal ablation. Third, while most acute LGE created by thermal ablation persisted in the chronic stage, the majority of acute LGE disappeared after PFA, despite durable PV isolation. Fourth, paralleling LGE changes, the wall compliance acutely declined in ablated regions after both PFA and thermal ablation, but recovered in the chronic stage only with PFA, leading to a recovery of LA reservoir and booster pump functions.

Acute tissue changes after ablation

At the acute stage after ablation, it is assumed that LGE both reflects myocyte necrosis and tissue oedema. Larger and more homogeneous acute LGE after PFA may be explained by its specific ablative mechanism. As PFA is not affected by the thermal conductivity of the tissue, pulsed field energy results in a homogeneous impact on the extensive tissue regardless of the tissue composition. The acute disruption of cell membranes after PFA enlarges the extracellular space,

potentially leading to higher gadolinium concentration. Another reason for homogeneous LGE after PFA is the avoidance of microvascular damage and intramural haemorrhage. This is consistent with pre-clinical studies reporting that PFA spares microvascular structures and induces no tissue haemorrhage.^{7,8} In contrast, microvascular damage and haemorrhage are common features after thermal ablation.¹⁰

Reversibility of late gadolinium enhancement after pulsed field ablation

One of the most intriguing findings with PFA is the disappearance of acute LGE in the chronic stage. This finding suggests low collagen synthesis after PFA because gadolinium contrast agents target areas with the rich extracellular matrix. Thermal ablation induces coagulative necrosis,¹⁴ triggering an inflammatory response with leucocytes.^{15,16} Once the inflammatory reaction is resolved, activated leucocytes facilitate collagen synthesis by promoting fibroblast activation.¹⁷ Thus, necrosis causes fibrosis through an inflammatory reaction. After PFA, the dominant mode of cell death is apoptosis, which does not trigger an inflammatory reaction.¹⁸ Another possible explanation for reduced chronic fibrosis after PFA derives from the preservation of the extracellular matrix architecture.^{7,8} Mechanosensitive signalling stimulates the transformation of fibroblasts into myofibroblasts, which promote fibrosis.¹⁹ After thermal ablation, the structural disruption of the matrix may expose fibroblasts to mechanical stress, leading to chronic fibrosis.²⁰ After PFA, the preserved extracellular matrix frame may protect fibroblasts from mechanical stress. The absence of microvascular structures destruction^{7,8} may also play a favourable role. By preserving wash-out kinetics, it allows better clearance of

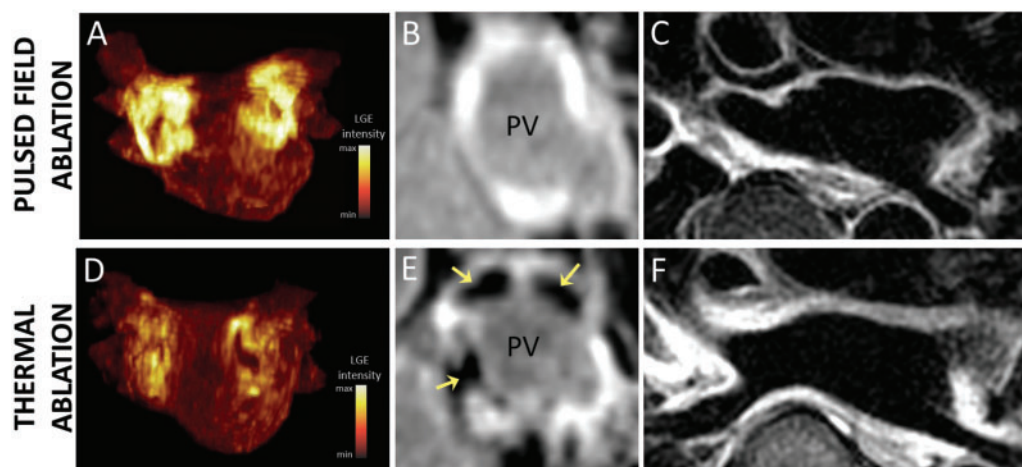


Figure 2 Examples of acute lesions on late gadolinium enhancement (LGE) and T2 imaging. (A–C) imaging after pulsed field ablation (PFA). (D–F) imaging after thermal ablation with radiofrequency energy. (A, D) maximum intensity projections of LGE volumes in anterior views. Acute LGE lesions were larger and more evenly distributed around pulmonary veins (PVs) after PFA (A) than after thermal ablation (D). (B, E) LGE images at the ostial level of the right superior PV. Acute LGE lesions after PFA (B) were more homogeneous than those after thermal ablation (E). Thermal ablation lesions showed dark areas within LGE (yellow arrows in E), consistent with intramural haemorrhage and/or microvascular damage. (C, F) Trans-axial T2 images showed oedema around PVs after both PFA (C) and thermal ablation (F), although slightly less after PFA.

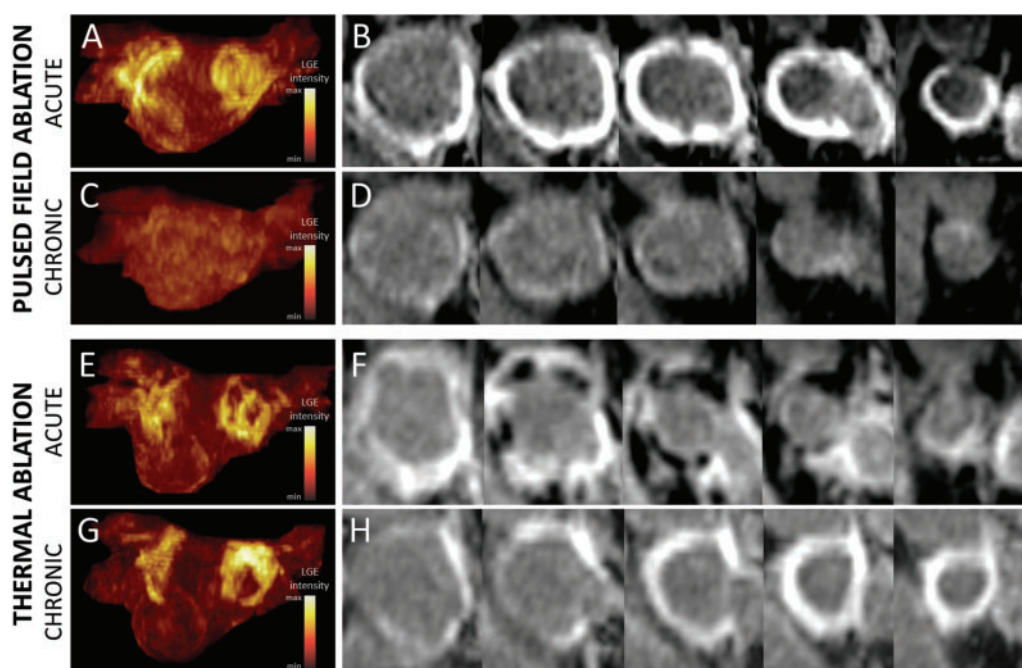


Figure 3 Reversibility of late gadolinium enhancement (LGE) in the chronic stage. (A–D) LGE imaging after pulsed field ablation (PFA). (E–H) LGE imaging after thermal ablation with radiofrequency energy. (A, C, E, G) maximum intensity projections of LGE volumes in posterior views (A, E: acute; C, G: chronic). (B, D, F, H) LGE image series perpendicular to the axis of the right superior pulmonary vein (PV), displayed from antral to ostial level (B, F: acute; D, H: chronic). After PFA, the majority of acute LGE lesions (A, B) had disappeared in the chronic stage (C, D). In contrast, after thermal ablation, most acute LGE lesions (E, F) persisted in the chronic stage (G, H).

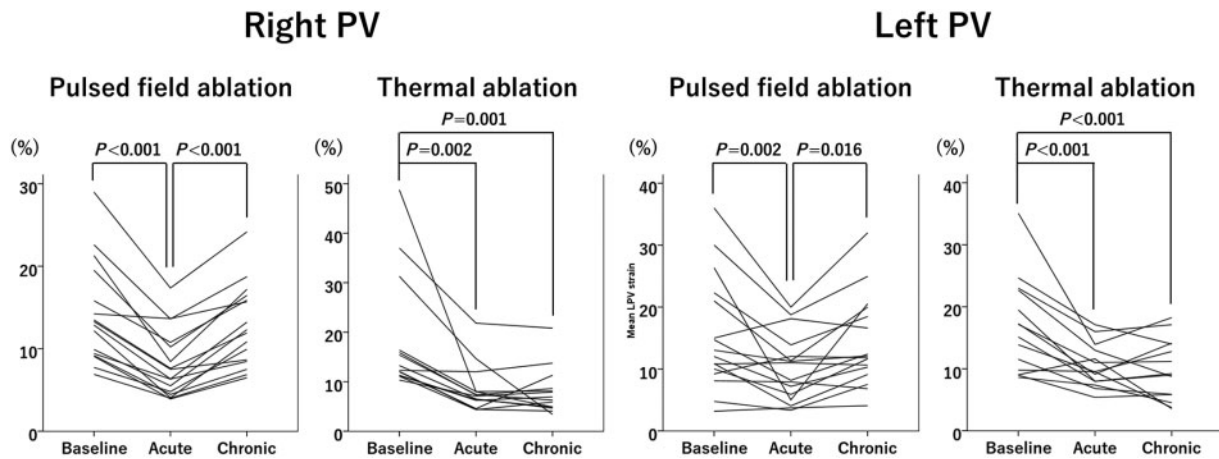


Figure 4 Maximum longitudinal strain values on the pulmonary vein (PV) antra. Changes in maximum longitudinal strain values in each patient of the pulsed field ablation (PFA) group and thermal group are shown.

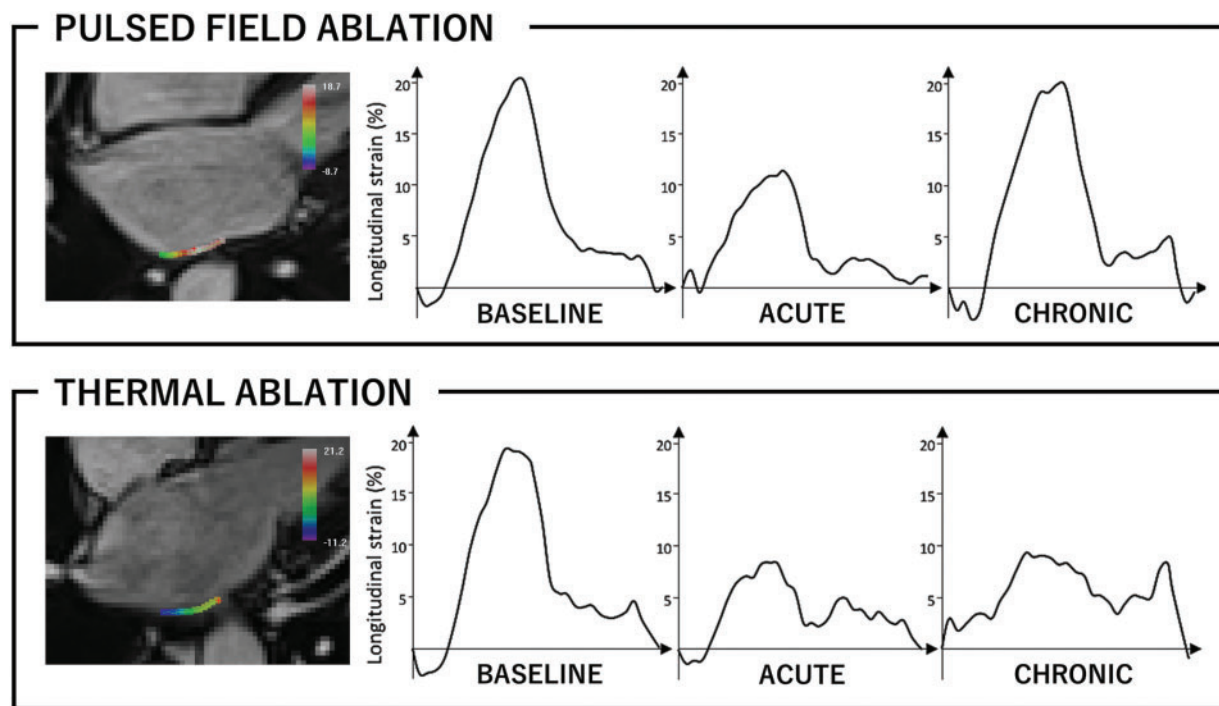


Figure 5 Examples of strain measurements on the left pulmonary vein (PV) antra. Top row: patient treated with pulsed field ablation (PFA). Bottom row: patient treated with thermal ablation by using radiofrequency energy. Note that the endocardial border of the PV antra is traced in the cine image (left panels in both rows). In the acute stage, the maximum strain decreased in both patients. In the chronic stage, it recovered to the baseline level after PFA, whereas it remained low after thermal ablation.

matrix debris in the acute stage, and of gadolinium contrast media in the chronic stage. Importantly, although LGE reversibility was constantly observed, no patient showed PV reconnection after PFA. Overall, our findings suggest that PFA can create durable lesions without inducing a fibrotic response.

Consequences on atrial function

In the acute stage, maximum strains of ablation sites declined after both PFA and thermal ablation. This is likely due to increased tissue stiffness caused by myocardial oedema. In the chronic stage, atrial strain remained altered with thermal ablation, while it recovered

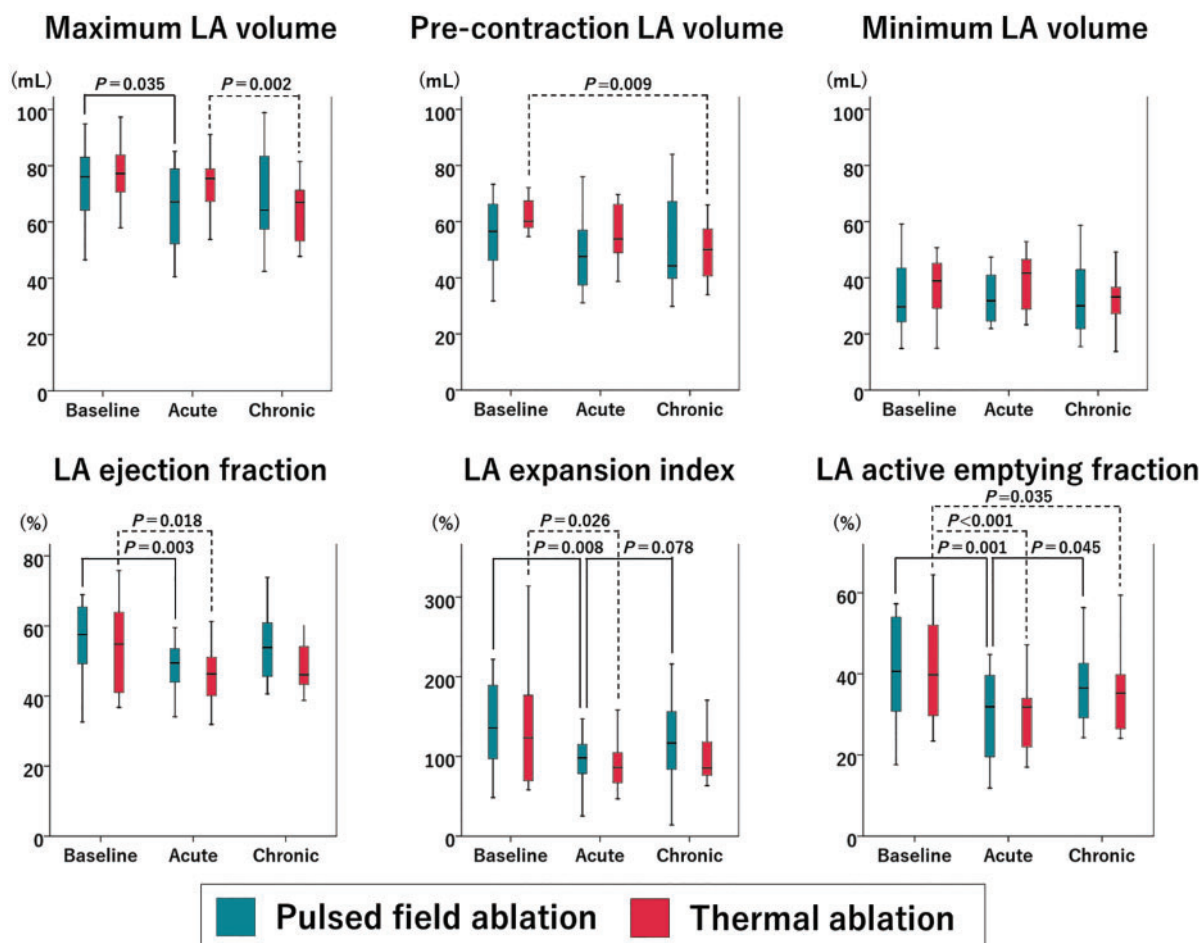


Figure 6 Left atrial (LA) volume and function parameters. Changes in LA volume and function parameters in the pulsed field ablation (PFA) group (green boxes) and the thermal group (red boxes) are shown.

with PFA, thus paralleling the evolution of LGE. A previous study has shown a spatial relationship between strain abnormalities and atrial fibrosis.²¹ Therefore, our results indicate that the reparative process without fibrosis may prevent myocardial stiffening after PFA.

Although the recovery of the maximum strain on the PV antra was too small to affect global atrial strain, an acute decline in the LA reservoir function recovered with PFA, as did the LA contractile function. Therefore, our results suggest that PFA preserves LA kinetic function via its specific reparative process involving reduced chronic fibrosis.

Clinical implications

The profibrotic response to ablation may be initially beneficial to reinforce the damaged myocardial tissue, but the excessive fibrosis results in myocardial stiffening and functional deterioration. Therefore, the non-fibrotic feature of PFA may bring superiority regarding cardiac function, which may prove especially useful in patients with heart failure. Moreover, the virtue of PFA on LA function may be more evident in patients with persistent AF, where more extensive ablation is often required. However, careful consideration is needed before applying this theory to clinical practice because the lack of chronic fibrosis may cause LA dilatation. Notably, in this study,

the LA volume decreased after PFA, suggesting that the reverse remodelling effect of AF suppression compensated for a potential LA dilatation effect of PFA.

Study limitations

This study has several limitations. First, this is a single-centre study with a relatively small sample size, which prevented us from analysing potential differences between different thermal ablation approaches. Second, LGE CMR methods only provide a relative contrast, and thresholding techniques applied to quantify baseline fibrosis and post-ablation scar are specific. Thus, current CMR methods do not allow a direct and quantitative comparison between both, and although no differences in baseline fibrosis were found between groups, it may have acted as a cofounder in the assessment of ablation lesions. Third, the strain measurement sites may have slightly differed between each time point because of changes in LA morphology and CMR slice positioning. Fourth, since the repeat mapping study was performed only in patients undergoing PFA, the relationship between CMR findings and electrophysiological properties after thermal ablation was not explored. Fifth, although durable PV isolation was observed in all eight patients treated with Biphasic 2

waveform in this study, the rate of durable PV isolation in patients treated with this waveform was lower in the IMPULSE/PEFCAT trials,⁶ which may reflect a selection bias.

Conclusions

Pulsed field ablation created larger and more homogenous acute tissue changes than thermal ablation, without causing microvascular obstruction and intramural haemorrhage. Furthermore, PFA induced less chronic LGE than thermal ablation, which suggested a specific reparative process with less chronic fibrosis. This process may have contributed to preserved tissue compliance in ablated areas, as well as LA reservoir and booster pump functions.

Supplementary material

Supplementary material is available at *Europace* online.

Funding

l'Agence Nationale de la Recherche (ANR) (Equipex MUSIC ANR-11-EQPX-0030, LIRYC ANR-10-IAHU-04); and the European Research Council (ERC no. 715093); the JHRS-EHRA Fellowship to Y.N.; the Canadian Institutes of Health Research Banting Postdoctoral Fellowship to F.D.R.; University of Basel, the Mach-Gaensslen foundation, and the Bangerter-Rhyner foundation to P.K.

Conflict of interest: H.C. has served as a consultant for Farapulse. V.Y.R. owns stock in Farapulse and has served as a consultant for Farapulse. P.J. owns stock in Farapulse and has received honoraria from Farapulse. C.E., C.S., and R.V. are Farapulse employees. The remaining authors have nothing to disclose.

Data availability

The data underlying this article cannot be shared publicly due to the privacy of individuals that participated in the study. The data will be shared on reasonable request to the corresponding author.

References

- de Gouveia RH, Melo J, Santiago T, Martins AP. Comparison of the healing mechanisms of myocardial lesions induced by dry radiofrequency and microwave epicardial ablation. *Pacing Clin Electrophysiol* 2006;**29**:278–82.
- Cochet H, Scherr D, Zellerhoff S, Sacher F, Derval N, Denis A et al. Atrial structure and function 5 years after successful ablation for persistent atrial fibrillation: an MRI study. *J Cardiovasc Electrophysiol* 2014;**25**:671–9.
- Kato R, Lickfett L, Meininger G, Dickfeld T, Wu R, Juang G et al. Pulmonary vein anatomy in patients undergoing catheter ablation of atrial fibrillation: lessons learned by use of magnetic resonance imaging. *Circulation* 2003;**107**:2004–10.
- Gibson DN, Di Biase L, Mohanty P, Patel JD, Bai R, Sanchez J et al. Stiff left atrial syndrome after catheter ablation for atrial fibrillation: clinical characterization, prevalence, and predictors. *Heart Rhythm* 2011;**8**:1364–71.
- Davalos RV, Mir IL, Rubinsky B. Tissue ablation with irreversible electroporation. *Ann Biomed Eng* 2005;**33**:223–31.
- Reddy VY, Neuzil P, Koruth JS, Petru J, Funosako M, Cochet H et al. Pulsed field ablation for pulmonary vein isolation in atrial fibrillation. *J Am Coll Cardiol* 2019;**74**:315–26.
- Koruth J, Kuroki K, Iwasawa J, Enomoto Y, Viswanathan R, Brose R et al. Preclinical evaluation of pulsed field ablation: electrophysiological and histological assessment of thoracic vein isolation. *Circ Arrhythm Electrophysiol* 2019;**12**:e007781.
- Koruth JS, Kuroki K, Iwasawa J, Viswanathan R, Brose R, Buck ED et al. Endocardial ventricular pulsed field ablation: a proof-of-concept preclinical evaluation. *Europace* 2020;**22**:434–9.
- Oakes RS, Badger TJ, Kholmovski EG, Akoum N, Burgon NS, Fish EN et al. Detection and quantification of left atrial structural remodeling with delayed-enhancement magnetic resonance imaging in patients with atrial fibrillation. *Circulation* 2009;**119**:1758–67.
- Cochet H, Mouriès A, Nivet H, Sacher F, Derval N, Denis A et al. Age, atrial fibrillation, and structural heart disease are the main determinants of left atrial fibrosis detected by delayed-enhanced magnetic resonance imaging in a general cardiology population. *J Cardiovasc Electrophysiol* 2015;**26**:484–92.
- McGann C, Kholmovski E, Blauer J, Vijayakumar S, Haslam T, Cates J et al. Dark regions of no-reflow on late gadolinium enhancement magnetic resonance imaging result in scar formation after atrial fibrillation ablation. *J Am Coll Cardiol* 2011;**58**:177–85.
- Karim R, Housden RJ, Balasubramaniam M, Chen Z, Perry D, Uddin A et al. Evaluation of current algorithms for segmentation of scar tissue from late gadolinium enhancement cardiovascular magnetic resonance of the left atrium: an open-access grand challenge. *J Cardiovasc Magn Reson* 2013;**15**:105.
- Lamacie MM, Thavendiranathan P, Hanneman K, Greiser A, Jolly MP, Ward R et al. Quantification of global myocardial function by cine MRI deformable registration-based analysis: comparison with MR feature tracking and speckle-tracking echocardiography. *Eur Radiol* 2017;**27**:1404–15.
- Dos Santos LF, Antonio E, Serra A, Venturini G, Okada M, Araújo S et al. Radiofrequency ablation does not induce apoptosis in the rat myocardium. *Pacing Clin Electrophysiol* 2012;**35**:449–55.
- Shinde AV, Frangogiannis NG. Fibroblasts in myocardial infarction: a role in inflammation and repair. *J Mol Cell Cardiol* 2014;**70**:74–82.
- Okoye AD, Tilley DG. Leukocyte-dependent regulation of cardiac fibrosis. *Front Physiol* 2020;**11**:301.
- Nakatani Y, Nishida K, Sakabe M, Kataoka N, Sakamoto T, Yamaguchi Y et al. Tranilast prevents atrial remodeling and development of atrial fibrillation in a canine model of atrial tachycardia and left ventricular dysfunction. *J Am Coll Cardiol* 2013;**61**:582–8.
- Szondi Z, Sarang Z, Kiss B, Garabuczi É, Köröskényi K. Anti-inflammatory mechanisms triggered by apoptotic cells during their clearance. *Front Immunol* 2017;**8**:909.
- Zhao XH, Laschinger C, Arora P, Szász K, Kapus A, McCulloch CA. Force activates smooth muscle alpha-actin promoter activity through the Rho signaling pathway. *J Cell Sci* 2007;**120**:1801–9.
- Hinz B, Phan SH, Thannickal VJ, Galli A, Bochaton-Piallat ML, Gabbiani G. The myofibroblast: one function, multiple origins. *Am J Pathol* 2007;**170**:1807–16.
- Peters DC, Duncan JS, Grunseich K, Marieb MA, Cornfeld D, Sinusas AJ et al. CMR-verified lower LA strain in the presence of regional atrial fibrosis in atrial fibrillation. *JACC Cardiovasc Imaging* 2017;**10**:207–8.